

# Increasing the efficiency of the Lesion segmentation tools to detect brain lesions in stroke

Mahsa Khorrampanah  
*department of electrical and computer  
 engineering  
 University of Tabriz  
 Tabriz, Iran  
 khorrampanah@tabrizu.ac.ir*

Ali Amani  
*department of electrical and computer  
 engineering  
 University of Tabriz  
 Tabriz, Iran  
 aliamani897@yahoo.com*

Maryam Yousefian  
*department of electrical and computer  
 engineering  
 University of Tabriz  
 Tabriz, Iran  
 maryam.yousefiann@gmail.com*

Hadi Seyedarabi  
*department of electrical and computer  
 engineering  
 University of Tabriz  
 Tabriz, Iran  
 seyedarabi@tabrizu.ac.ir*

**Abstract**—Stroke is the principal cause of death all over the world. Lesion detection is a crucial step in diagnosis and therapy of patients with stroke lesion. MRI is useful device in lesion segmentation that produces different brain image series, such as T1, T2 and FLAIR. Nowadays, automatic methods for detecting lesion are preferable to semi-automatic methods due to their speed, flexibility and availability. So, the efficiency of these methods in detecting lesion is important. LST-Lesion segmentation tool by SPM is an automatic tool which is most commonly used to detect Multiple Sclerosis (MS) lesions. Moreover, the LST has been investigated for detecting of stroke lesions. In this study the operation of this tool is examined both in the old version (SPM8) and the new one (SPM12) in a wide range of lesion volumes of ischemic stroke. The results show that LST can be used as an automated tool for detecting of stroke lesions but it works better in old version. Also, the performance of the LST in detection of lesions is improved by two feature maps. These feature maps separate missed and abnormal pixels. These two properties have more effects in detection of large lesions which are detected with high quality.

**Keywords**—segmentation, stroke lesion, LST, SPM

## I. INTRODUCTION

Every year, millions of people all over the world suffer from stroke. It often occurs in the elderly and usually disrupts some activities in patient's body. These disorders are caused by lesions in different parts of the head.

Consequently, lesion detection is one of the important steps in researching stroke. Recent developments in neuroimaging methods caused by the further inspection of the human brain. MRI Brain image segmentation is a noteworthy tool in the diagnosis and therapy of many different types of brain damages. It provides high effective representation in discerning among the different forms of this disorder. Therefore, researchers usually use it in different studies. Over the last two decades, MRI has gone key not only for the assessment and monitoring of stroke, but also as an endpoint for clinical testing. But, detecting the lesion from MRI images is still a challenging problem.

Recently, many types of research were done for designing tools and methods of lesion detection. Support vector machines (SVM) [1], Markov random field (MRF) classifier [2], K-nearest neighborhood (KNN) classifier [3,4] and likelihood estimator [5] are several methods that, were used for detecting of various lesions.

One of the strong tools in lesion segmentation is the Lesion segmentation tool (LST) [6] (<http://www.applide-statistics.de/lst.htm>) which was validated on MS lesion detection during the time. But the validity of this tool is not specified in stroke lesion detection.

In this paper, we investigated the performance of the LST tool for detection of a wide range of stroke lesion volumes of MRI scans to verify or falsify the LST tool in stroke lesion detection. Then, using two feature maps made by Griffis et al. [7], we calculated the missing and abnormal pixels and changed the feature map of lesion detection in LST. Then, using the new feature map, the performance of the LST tool was improved extensively.

## II. MATERIALS AND METHODS

### A. Dataset

For this research, datasets of ischemic stroke lesion segmentation (ISLES) in 2015, has been used. This challenge has two types of datasets as sub-acute ischemic stroke lesion segmentation (SISS) and acute stroke outcome/penumbra estimation (SPES) [8]. More information is available in <http://www.isles-challenge.org/ISLES2015>.

The SISS is used in this research, which includes 28 training and 36 test MRI datasets. Also, the training samples have been used with FLAIR and T1 strings.

### B. Lesion Segmentation Tools

In 2012, automatic detection of the lesion using LST was designed by Smith et al.. This tool was initially used to detect lesions in 53 patients with MS, but due to its high performance, it was used to detect other lesions, including stroke lesion diagnosis. LST works with SPM software, and the initial version includes a lesion detection with Lesion growth algorithm (LGA) in the SPM8 software

(<http://www.fil.ion.ucl.ac.uk/spm/software/spm8>). In 2015, the new version of LST was designed, which is available on <http://www.fil.ion.ucl.ac.uk/spm/software/spm12>. The new version, in addition to LGA, includes the Lesion prediction algorithm (LPA). In the following, we describe each of these three algorithms (LGA-SPM8, LGA-SPM12, LPA) with their usage in lesion detection.

#### 1) Lesion growth algorithm based on SPM8 (LGA SPM8)

This algorithm was proposed in [6] and consists of three main steps. The first step is pre-processing, that two T1 and FLAIR MRI images are taken to SPM8 software. In this step, the T1 image is classified into three layers of GM<sup>1</sup>, WM<sup>2</sup> and CSF<sup>3</sup>. The FLAIR image is co-registered after the Bias-correction with the T1 image.

In the second step, a primary map of the lesion is provided. In this phase, using the PVE<sup>4</sup> image [6], the FLAIR image density distribution is obtained for each region (GM, WM, and CSF).  $p_0$  is a number between 1 and 3, which assigns a number for each pixel. So, the FLAIR image is scaled according to the density distribution  $p_0$ . Perhaps with this scaling, the pixels of the lesion exhibit abnormal behavior.

An initial map of the lesion for each pixel in each area ( $b_k$ ) is obtained from the differences of each scaled pixel in the FLAIR image ( $y_i$ ) and the average of the scaled pixels in that area ( $y_i - \bar{y}_k$ ). Then the results are multiplied by  $p_0$  value in that area and the possibility of being the lesion in the white matter region (atlas\_wm). Thus, a primary map of the lesion in each area is obtained ( $B_k = \{b_1, \dots, b_i, \dots, b_n\}$ ).

Eventually, the primary lesion map in each area is added, and the primary map of the lesion is created. According to the equation (1), the primary map of the lesion is B, which consists of three parts: primary map of the lesion of white matter ( $B_{wm}$ ), primary map of the Gray matter lesion ( $B_{gm}$ ) and primary map of the cerebrospinal fluid lesion ( $B_{csf}$ ). The primary map of the lesion for these three parts are shown in the equations (2), (3) and (4).

$$B = B_{gm} + B_{wm} + B_{csf} \quad (1)$$

$$B_{wm} = p_0 (p_0 > 2.5) (f2\_norm - mean\_wm) atlas\_wm \quad (2)$$

$$B_{gm} = p_0 (p_0 > 1.5 \& p_0 < 2.5) (f2\_norm - mean\_gm) atlas\_wm \quad (3)$$

$$B_{csf} = p_0 (p_0 < 1.5 \& p_0 > 0) (f2\_norm - mean\_csf) atlas\_wm \quad (4)$$

$f2\_norm$  is the normalized image of the FLAIR image. The  $mean\_wm$ ,  $mean\_gm$ , and  $mean\_csf$  are the mean spacing of white matter pixels, gray matter, and cerebrospinal fluid of  $f2\_norm$ . The binary mode of lesion's initial map is obtained by thresholding on the GM layer.

The final step is the improvement of the primary map. The neighbor pixels of the lesion are analysed using defined conditions. This procedure is applied iteratively on the primary map of the lesion for all pixels. Fig. 1 shows the block diagram of the LGA-SPM8.

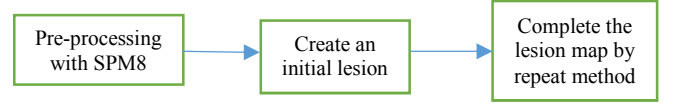


Fig. 1. Block diagram of the SPM8 LGA

#### 2) Lesion growth algorithm based on SPM12 (LGA SPM12)

The main steps of this algorithm are the same as the previous version, but the pre-processing on the T1 images and the acquisition of different layers are using SPM12.

#### 3) Lesion prediction algorithms based on SPM12 (LPA SPM12)

This algorithm only uses FLAIR images. The block diagram of the LPA algorithm is shown in Fig. 2.

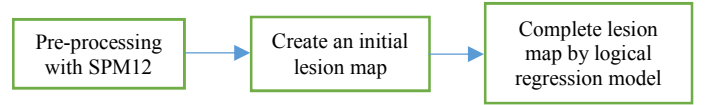


Fig. 2. Block diagram of the LPA algorithm

### C. Proposed Method

In [9] it was studied on the 50 patients with MS, it was found that LST would be better in the older version of the SPM and more likely to detect the lesion with more Dice coefficient [10]. At [9] the mean Dice in MS lesion detection for LGA-SPM8, LGA-SPM12 and LPA-SPM12 were calculated 0.60, 0.53 and 0.57 respectively.

In this study, by computing parameters such as Dice on training datasets of stroke patients, the results are similar to the results of [9]. Therefore, in addition to evaluating and comparing the performance of the LST in the diagnosis of the stroke lesions, tried to improve the performance of the LST with the new version, which works on SPM12.

For this aim, the function of this algorithm was improved by adding two features to the primary map of the lesion (B) in the LGA-SPM12 algorithm. To create each of these features, T1 segmented images were categorized into three regions like white matter, gray matter and cerebrospinal fluid in the LGA-SPM12 (PPM<sup>5</sup>). Then, the coded images of three regions white matter, gray matter and cerebrospinal fluid are used in the lesion-GNB algorithm (TPM<sup>6</sup>). The definitions of the TPM and PPM are at [7] in details.

Unified normalization [7] is a suitable method for normalizing the brain with the lesion. So the cost-function masking does not require [11,12]. The TPM is obtained using the unified normalization method with the new segment tool in the SPM12. In the following, TPM and PPM are divided into two areas, the affected and unaffected.

The first feature is based on the fact that, SPM typically detects the tissues of the missing lesion with the low probability of white matter or gray matter in the cerebrospinal fluid [13,14,15]. For each pixel of the lesion, the first feature map (equation (7)) is obtained using the following equation:

<sup>1</sup> Gray matter

<sup>2</sup> White matter

<sup>3</sup> Cerebrospinal fluid

<sup>4</sup> Partial volume effect

<sup>5</sup> Prior probability map

<sup>6</sup> Tissue probability map

$$f11 = (csf_u \times gm_a + csf_u \times wm_a + csf_a \times gm_u + csf_a \times wm_u) - (csf_u \times gm_u + csf_u \times wm_u + csf_a \times gm_a + csf_a \times wm_a) \quad (5)$$

$$f12 = (csf_p \times gm_a + csf_p \times wm_a + csf_a \times gm_p + csf_a \times wm_p) - (csf_p \times gm_p + csf_p \times wm_p + csf_a \times gm_a + csf_a \times wm_a) \quad (6)$$

$$f1 = (f11 + f12)/2 \quad (7)$$

The second feature is based on the fact that the SPM recognizes abnormal tissues of the gray matter in T1 images as healthy tissues of the gray matter [16]. For each pixel in the region containing the lesion, the second feature map is obtained as equation (10).

$$f21 = (gm_a \times wm_u + gm_u \times wm_a) - (gm_a \times wm_a + gm_u \times wm_u) \quad (8)$$

$$f22 = (gm_a \times wm_p + gm_p \times wm_a) - (gm_a \times wm_a + gm_p \times wm_p) \quad (9)$$

$$f2 = (f21 + f22)/2 \quad (10)$$

In the equations (5 to 10)  $gm_a$ ,  $csf_a$  and  $wm_a$  are the affected pixels in the gray matter region, spinal fluid and white matter. The regions with u index, contain unaffected pixels and with the p index, representing the prior pixels.

Subsequently, the first feature is the missed pixels of the white matter and the gray matter. The second feature is related to abnormal gray matter pixels. These two properties are applied to the initial map of the lesion in equations (2) and (3). As a result, equations (2) and (3) converted to equations (11) and (12). In the following, the initial map of the lesion will be obtained from equation (13).

$$B1_{wm} = p0(p0 > 2.5)(f2_{norm} - mean_{wm})atlas_{wm} + p0(p0 > 2.5)f1 \quad (11)$$

$$B1_{gm} = p0(p0 > 1.5 \& p0 < 2.5)(f2_{norm} - mean_{gm})atlas_{wm} + p0(p0 > 1.5 \& p0 < 2.5)(f2 + f) \quad (12)$$

$$B = B1_{gm} + B1_{wm} + B_{csf} \quad (13)$$

Fig. 3 and Fig. 4 show the performance of LGA algorithms of LST and proposed method for stroke lesion detection in two datasets compared with manual mode.

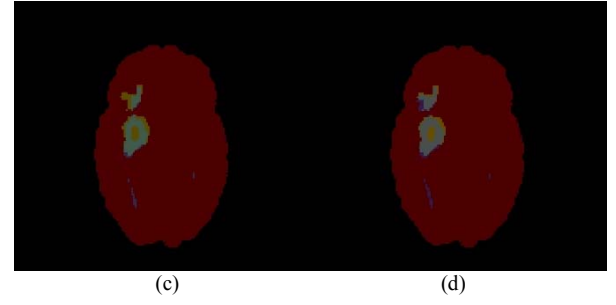
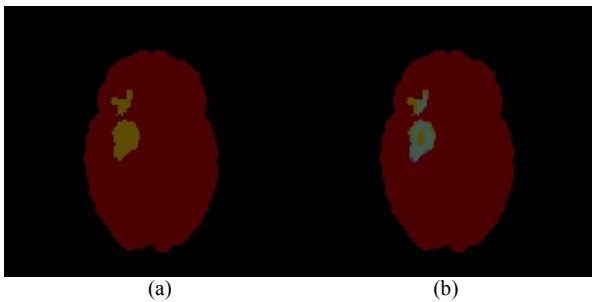


Fig. 3. Stroke lesion detection in the first data: a) manual mode, b) comparing of the LGA SPM8 and manual mode, c) comparing of the LGA SPM12 and manual mode, d) comparing of the proposed work and manual.

• manual, Overlap, Segmented

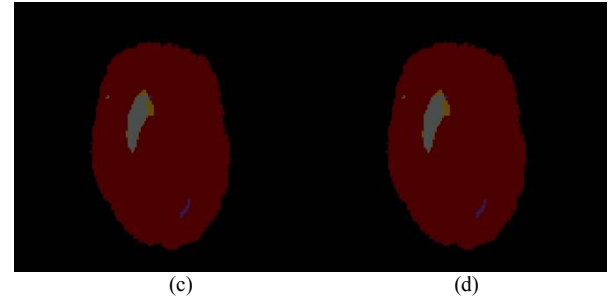
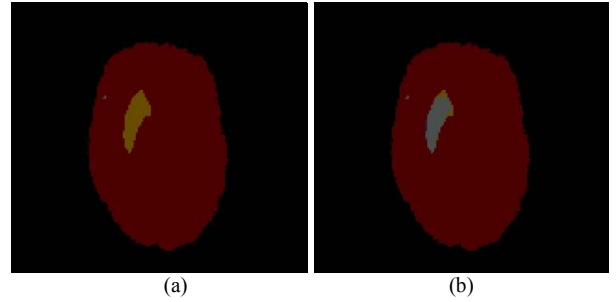


Fig. 4. Stroke lesion detection in second data: a) manual mode, b) comparing of the LGA SPM8 and manual mode, c) comparing of the LGA SPM12 and manual mode, d) comparing of the proposed work and manual.

• manual, Overlap, Segmented

In order to achieve the performance of these three algorithms, it is necessary to calculate the performance of these three algorithms in the diagnosis of the lesion relative to the manual state. The performance is determined by the Dice parameter [14]. This parameter is the overlap of the segmented lesion pixels and manual mode and is calculated by equation (14).

$$Dice = 2 \times TP / (2 \times TP + FN + FP) \quad (14)$$

In equation (14), TP, FN and FP are true positive, false negative and false positive respectively [17].

### III. RESULTS

In this section, we will calculate and compare the various factors to achieve the performance of algorithms LGA-SPM8, LGA-SPM12, LPA and the proposed method in diagnosis of stroke.

The performance of these four algorithms in large lesions (bigger than 15 ml) and small lesion (smaller than 15 ml) is examined. The Dice parameter is used to evaluate performance of three LST algorithms and the proposed method. Table 1, shows average Dices in ISLES 2015 training datasets for LGA-SPM8, LGA-SPM12, and LPA. The average Dices for the total of 28 training datasets in the LGA-SPM8 is higher than LGA-SPM12, and the LPA performance is lower than others. Also, the proposed method has the higher total average Dices than others.

If we classify the datasets based on the size of their lesions, the average Dices in the large lesions in the LGA-SPM8 is higher than its new version. But in small lesions, the new LGA (LGA-SPM12) outperforms its old version. The proposed method doesn't improve dramatically in small lesions, but shows great improvement in the large lesions. The LPA algorithm is weak in detecting small lesions of the stroke, but in detecting large lesions the average Dice is comparable with the rest of the algorithms.

Table 2 shows the average sensitivity in four algorithms, the overall average sensitivity of the proposed method has been greatly improved. The LGA in the new version has a higher overall average sensitivity than its older version, and the LPA has a lower average sensitivity than the others. In datasets with small lesions, the average sensitivity in the new version of LGA is higher than its old version, and the LPA works better than the LGA. Also, the improvement of the average sensitivity in the proposed method is not impressive comparing to LGA. In datasets with large lesions, the average sensitivity of the LGA in the old version is higher than its new version. Also, the improvement of average sensitivity of the proposed method is significant compared to the LGA.

Table 1. Average of Dices on training datasets of stroke patients.

Method	Total (n=28)	(n=14)<15ml	(n=14)>15ml
LGA-SPM8	0.56	0.30	0.43
LGA-SPM12	0.51	0.31	0.41
LPA	0.47	0.20	0.34
Proposed method	0.61	0.32	0.48

Table 2. Average Sensitivity on training datasets of stroke patients.

Method	Total (n=28)	(n=14)<15ml	(n=14)>15ml
LGA-SPM8	0.43	0.35	0.51
LGA-SPM12	0.44	0.38	0.49
LPA	0.39	0.39	0.40
Proposed method	0.52	0.39	0.62

#### IV. DISCUSSION

Automatic stroke lesion detection methods are fast, flexible and more accessible than manual and semi-automatic methods. The goal of this study is to validate the LST to detect stroke lesions and this validation is not limited to a specific volume of stroke lesion and it has been studied in a wide range of stroke lesions (from 207.964 ml to 0.074 ml).

This automatic tool was designed in 2012 by Smith et al. to diagnose MS lesions. In 2017, Egger et al. evaluated the validity of this tool on 50 patients with MS lesions and compared the performance of this tool with three algorithms LGA-SPM8, LGA-SPM12 and LPA and three manual methods.

The validity of the LST tool in diagnosis of stroke is evaluated by examining the performance of these three algorithms in different volumes of stroke lesions. In this study the primary map of the lesion was modified in LST to improve its performance in diagnosis of the lesions using two features which detected missed pixels and abnormal pixels.

#### A. Dice coefficient and sensitivity of automated methods

As shown in Table 1, the performance of LGA in an old version that works with the SPM8 is better than its new version. We use 28 samples of ISLES 2015 datasets. 14 samples have small lesions (smaller than 15 ml) and the others have large lesions (bigger than 15 ml). As shown in Table 1, the performance of LGA on large lesions in the older version is better than the new one. As shown in Table 2, the LGA-SPM8 performs better in diagnosing large lesions comparing to its new version. Also, the LPA has lower performance compared to both versions of the LGA in detecting large and small lesions. The proposed method has more effective performance in identifying large and small lesions. Improved performance in detecting a large lesion is remarkable.

#### B. Performance comparing to the similar methods

To compare LST algorithm and proposed work with similar methods, recent works were selected that used our datasets. Kaiser et al. [18] used random forest method and features like entropy and gradient to classify and diagnose ischemic stroke lesions. The mean value of Dices coefficient on ISLES 2015 training dataset was 0.54 [18]. J. Muschelli [19] used method of random forest for detecting stroke lesion by using some features for separating damaged areas from healthy tissue. In this case, the mean value of Dices Coefficient on ISLES 2015 training dataset was 0.48 [19]. Jesson et al. [20] prepared a hierarchical framework that separated the damaged and healthy structures in the MRI images. The mean value of Dices Coefficient on ISLES 2015 training dataset in this algorithm was 0.45 [20].

#### V. CONCLUSION

In this paper, the efficiency of the LST was evaluated using three algorithms LGA-SPM8, LGA-SPM12 and LPA in the brain lesion detection for the ischemic stroke. The results showed the LST is a suitable tool in stroke lesion detection. In this study, an algorithm containing two feature maps was proposed for the high-quality diagnosis of the lesions. In this algorithm, the missing and the abnormal pixels were added to the LGA map with proper weighting for each area. The results on ISLES2015 datasets using LST and proposed algorithm showed that the proposed method has high performance in different volumes of the ischemic stroke lesions and increased the efficiency of the LST.

#### FUTURE WORKS

In this work, the performance of the LST was improved in large volumes of the stroke lesions (more than 15ml). The

research team will focus on lesion maps which will be applied on feature maps to improve detection of the small lesions.

## REFERENCES

- [1] R. J. Ferrari, X. Wei, Y. Zhang, J. N. Scott, J. R. Mitchell, "Segmentation of multiple sclerosis lesions using support vector machines," *Proceedings of SPIE*, vol. 5032, pp. 16-26, 2003.
- [2] L. Li, X. Wei, X. Li, S. Rizvi, Z. Liang, "Mixture segmentation of multispectral MR brain images for multiple sclerosis," *Journal of systemics*, vol. 3, pp. 65-68, 2005.
- [3] P. Anbeek, K. L. Vincken, M. J. van Osch, R. H. Bishops, J. van der Grond, "Probabilistic segmentation of white matter lesions in MR imaging," *Neuroimage*, vol. 21, pp. 1037-1044, 2004.
- [4] Y. Wu, S. K. Warfield, I. L. Tan, W. M. Wells, D. S. Meier, R. A. van Schijndel, F. Barkhof, C. R. Guttmann, "Automated segmentation of multiple sclerosis lesion subtypes with multichannel MRI," *Neuroimage*, vol. 32, pp. 1205-1215, 2006.
- [5] L. S. Ait-Ali, S. Prima, P. Hellier, B. Carsin, G. Edan, C. Barillot, "STREM: the robust multidimensional parametric method to segment MS lesions in MRI," *Medical image computing and computer-assisted intervention-Miccai*, pp. 409-416, 2005.
- [6] P. Schmidt, C. Gaser, M. Arsic, D. Buck, A. Forschler, A. Berthele, M. Hoshi, R. Ilg, V. J. Schmid, C. Zimmer, B. Hemmer, M. Muhlau, "An automated tool for detection of FLAIR-Hyperintense white matter lesions in multiple sclerosis," *Neuroimage*, vol. 59, pp. 3774-3783, 2012.
- [7] J. C. Griffis, J. B. Allendorfer, J. P. Szaflarski, "Voxel based Gaussian naïve bayes classification of ischemic stroke lesions in individual T1-weighted MRI scans," *Journal of neuroscience methods*, vol. 257, pp. 97-108, 2016.
- [8] O. Maier, B. H. Menze, J. von der Goblentz, L. Hani, M. P. Heinrich, et al., "ISLES 2015- A public evaluation benchmark for ischemic stroke lesion segmentation from multispectral MRI," *Medical Image Analysis*, vol. 35, pp. 250-269, 2017.
- [9] C. Egger, R. Opfer, C. Wang, T. Kepp, M. P. Sormani, L. Spies, M. Barnett, S. Schippling, "MRI FLAIR lesion segmentation in multiple sclerosis: Does automated segmentation hold up with manual annotation?," *Neuroimage: Clinical*, vol. 13, pp. 264-270, 2017.
- [10] L. R. Dice, "Measures of the amount of ecologic association between species," *Ecology*, vol. 26, pp. 297-302, 1945.
- [11] J. Crinion, J. Ashburner, A. Leff, M. Brett, C. Price, K. Friston, "Special normalization of lesioned brains: performance evaluation and impact on fMRI analyses," *Neuroimage*, vol. 37, pp. 866-75, 2007.
- [12] P. Ripolles, J. Marco-Pallares, R. de Diego-Balaguer, J. Miro, M. Falip, M. Juncadella, et al., "Analysis of automated methods for spatial normalization of lesioned brains," *Neuroimage*, vol. 60, pp. 1296-306, 2012.
- [13] M. L. Seghier, A. Ramackhansingh, J. Crinion, A. P. Leff, C. J. Price, "Lesion identification using unified segmentation-normalisation models and fuzzy clustering," *Neuroimage*, vol. 41, pp. 1253-66, 2008.
- [14] M. Wilke, M. Staudt, H. Juenger, W. Grodd, C. Braun, I. Krageloh-Mann, "Somatosensory system in two types of motor reorganization in congenital hemiparesis: topography and function," *Hum brain map*, vol. 30, pp. 776-88, 2009.
- [15] M. Wilke, H. B. De, H. Juenger, H. O. Karnath, "Manual, semi-automated and automated delineation of chronic brain lesions: a comparison of methods," *Neuroimaging*, vol. 56, pp. 2038-46, 2011.
- [16] S. Mehta, T. J. Grabowski, Y. Trivedi, H. Damasio, "Evaluation of voxel based morphometry for focal lesion detection in individuals," *Neuroimage*, vol. 20, pp. 1438-54, 2003.
- [17] K. H. Zou, S. K. Warfield, A. Bharatha, C. M. C. Tempany, M. R. Kaus, S. J. Haker, et al., "Statistical validation of image segmentation quality based on a spatial overlap index1," *Acad Radiol*, vol. 11, pp. 178-189, 2004.
- [18] M. Qaiser, A. Basit, "Automatic ischemic stroke lesion segmentation in multi-spectral MRI images using random forests classifiers," *Springer*, vol. 9556, pp. 266-274, 2015.
- [19] (2015) The ISLES website. [Online]. Available: <http://www.isles-challenge.org/ISLES2015/articles/muscj1.pdf>.
- [20] (2015) The ISLES website. [Online]. Available: <http://www.isles-challenge.org/ISLES2015/articles/jessa3.pdf>.